TITLE

Reactive Oxygen Detoxification Contributes to *Mycobacterium abscessus* Antibiotic Survival

AUTHORS

Nicholas A. Bates[1,2], Ronald Rodriguez[3,4], Rama Drwich[1], Abigail Ray[5], Sarah A. Stanley[3], Bennett H. Penn[1]*

AFFILIATIONS:

1. Department of Internal Medicine, University of California, Davis, Davis, California, United States of America
2. Graduate Group in Immunology, University of California, Davis, Davis, California, United States of America
3. Department of Molecular & Cell Biology, University of California, Berkeley, California, USA
4. Department of Plant & Microbial Biology, University of California, Berkeley, California, USA
5. Microbiology Graduate Group, University of California, Davis, Davis, California, United States of America

*Corresponding author

Email: bhpenn@ucdavis.edu

ABSTRACT

It has long been recognized that when a population of bacteria are exposed to a bactericidal antibiotic the majority of the population rapidly dies, but that a sub-population of cells, known as “persister cells” can survive for prolonged periods in a non-growing, but viable, state and can resume replication upon removal of the antibiotic. Persister cell frequency is dramatically

increased by stress such as nutrient deprivation, but it is unclear how what pathways enable survival and how the process is regulated and enhanced by environmental stress. Mycobacterial persisters are particularly resilient, with the ability to endure many weeks of antibiotic exposure. To identify the genetic determinants of persister cell survival we carried out a transposon mutagenesis coupled with high-throughput sequencing (Tn-Seq) screen in *Mycobacterium abscessus* (*Mabs*). We identified a number of pathways contributing to persister cell survival, including the bacterial proteasome and enzymes needed to detoxify reactive oxygen species (ROS). We showed that *MAB_2470c*, encoding the KatG catalase/peroxidase was required for both spontaneous and starvation-induced persister cell formation in response to multiple antibiotics. Consistent with a role for ROS in antibiotic-mediated cell death we observed an accumulation of ROS following antibiotic exposure. We tested the role of oxygen in bacterial death, and found that that hypoxic conditions significantly impaired bacterial killing, and notably, in the absence of oxygen KatG became dispensable. Taken together, these findings support a model where the lethality of some antibiotics are enhanced by the accumulation of ROS.

INTRODUCTION

A key goal of antibiotic therapy is eradication of the pathogenic bacteria. While many common infections respond well to antibiotics, and high cure rates are achieved with 1-2 weeks of therapy[1, 2], there are also infections where bacterial eradication is either very slow, or frequently incomplete. This challenge is exemplified by mycobacterial infections, where treatment courses extend from months to years to prevent relapse.

While the ability of mycobacteria to escape antibiotic-mediated killing is multifactorial, the phenomenon of antibiotic “persistence” is likely to be an important contributor[3-6]. Studies on penicillin dating from the 1940s noted that while the majority of a susceptible bacterial population died rapidly over a few hours, a small sub-population of ‘persisters’ remained viable for over a

53 week[7]. Importantly, these persister cells had not acquired a mutation conferring heritable antibiotic
54 resistance, and do not grow in the presence of the antibiotic. Rather, they have entered into a
55 readily-reversable epigenetic state[8-10] where despite antibiotic-mediated inhibition of critical
56 processes, they are able to survive. Virtually all bacteria display the ability to form persister cells,
57 and persister cell development is strongly induced in response to stresses such as nutrient
58 deprivation or acidic pH[6, 7, 11, 12]. Notably, these same stresses are encountered in the lysosome
59 of an activated immune cell[13], and studies of pathogens isolated from activated macrophages
60 indeed show a strong immune-mediated increase in persister cells[5, 14]. Thus, paradoxically, the
61 immune system may actually impede bacterial eradication by antibiotics.
62
63 Persister formation has been studied extensively in model systems such as *Escherichia coli* ,
64 providing important insights, but also highlighting some of the uncertainties of current models for
65 this process. Several different pathways have been implicated in persister formation in *E. coli*
66 including the HipBA toxin-antitoxin system[15] that regulates translation, ppGpp synthesis by
67 RelA/SpoT enzymes[16, 17], and Lon protease[16]. In each of these models, the postulated effect is to
68 arrest cell division and render the process targeted by antibiotics non-essential. However,
69 important questions remain unanswered. It is unclear how the process is regulated and induced
70 by stress. It is also unclear how some bacterial cells survive when critical processes such as
71 transcription or translation are arrested by antibiotics.
72
73 Even the mechanism of cell death following antibiotic exposure itself remains uncertain, and
74 somewhat controversial. Historically, antibiotics have been assumed to kill bacteria as a direct
75 result of inhibition of their target molecules. For example, β-lactam antibiotics directly disrupt cell
76 wall integrity leading to mechanical cell lysis[18]. However, a number of studies have suggested
77 that reactive oxygen species (ROS) accumulation triggered by antibiotic stress downstream of

78 target inhibition might also contribute to cell death[10,19, 20]. However, other studies have found no
79 such association[21, 22], leaving the role of ROS in antibiotic-mediated cell death unresolved.
80
81 Studying persister cell physiology in mycobacterial pathogens offers several advantages.
82 Mycobacterial persister cells are particularly resilient, as *Mycobacterium smegmatis* (*Msmeg*) and
83 *Mycobacterium tuberculosis (Mtb)* persisters can endure many weeks of antibiotic exposure[10, 23,
84 24], and clinically, mycobacterial infections are difficult to eradicate. Fully-susceptible *Mtb* requires
85 multiple antibiotics for four months or longer[25 26], whereas non-tuberculous mycobacteria typically
86 require treatment for 12-18 months, and have a relapse rates of roughly 50%[27]. Treatment of
87 *Mycobacterium abscessus* (*Mabs*) is particularly challenging. In addition to the possibility of
88 forming persister cells, it is intrinsically resistant to many classes of antibiotics, leaving few
89 treatment options. This leads to the use of antibiotics with greater toxicity to patients, and a need
90 to use these agents for prolonged periods to prevent relapse[28].
91
92 Previous genetic screens have studied antibiotic responses in mycobacteria, with some
93 evaluating heritable resistance, and others investigating persister cell formation. Several studies
94 of genetic resistance have successfully used either transposon mutagenesis with high-throughput
95 sequencing of insertion sites (Tn-Seq) or CRISPR-based transcriptional repression with high-
96 throughput sequencing of guide RNAs (CRISPRi) to identify genes promoting growth in sub-
97 inhibitory concentrations of antibiotic. These studies have provided insights such as the
98 importance of cell membrane permeability controlling antibiotic penetration into the cytoplasm[29-
99 31].
100 The reversable state of persister cell formation has proven challenging to study, likely due to the
101 effects of widespread bacterial cell death during the experiment, which creates population
102 bottlenecks that obscure mutant phenotypes[32, 33 ,34.] There has been one highly-effective Tn-Seq

103 study of rifampin-specific antibiotic tolerance in *Mtb* that successfully isolated over 100 mutants[19],
104 demonstrating the feasibility of genetic screening in this context. However, whether these
105 phenotypes seen with rifampin in *Mtb* extend to other organisms and other antibiotics remains to
106 be determined.
107
108 Here, we study the process of persister cell formation in *Mabs*, and describe the results of a
109 genome-wide genetic screen seeking to identify genes required for both spontaneous and
110 starvation-induced persister cell formation in *Mabs*. We identified a number of pathways
111 contributing to persister cell survival and identified the KatG catalase-peroxidase ROS detoxifying
112 enzyme as conferring the ability to survive for prolonged periods in several antibiotics, providing
113 support for the idea that reactive oxygen species can indeed contribute to bacterial cell death
114 from antibiotics.
115
116 **RESULTS**
117 **Starvation-induced persister cell formation in mycobacteria**
118 We first sought to develop conditions suitable for genetic analysis of antibiotic tolerance in
119 mycobacteria. Genetic screens examining persister cell formation face two inherent obstacles.
120 First, cell death during the experiment creates population bottlenecks that obscure mutant
121 phenotypes. In addition, most mycobacterial populations contain spontaneous drug-resistant
122 mutants that can expand if the population is exposed to a single antibiotic. To overcome these
123 obstacles, we sought to establish large-scale, high-density culture conditions that still maintained
124 antibiotic potency.
125
126 We began by assessing the feasibility of this approach using wild-type *Msmeg,* exposing the cells
127 to either a combination of two antibiotics routinely used to treat *Mabs* infections, tigecycline and

128 linezolid (TIG/LZD)[27, 35], or to the combination of rifampin, isoniazid, and ethambutol
129 (RIF/INH/EMB) used to treat *Mtb*. We first determined the minimum-inhibitory concentrations
130 (MICs) and minimum bactericidal concentrations (MBCs) of cultures at the standard density used
131 in clinical laboratories for mycobacterial drug-susceptibility testing versus the high-density
132 conditions that would be needed for genetic analysis of antibiotic persister cells. We established
133 the MIC and MBC at the standard 5E5 colony-forming units (CFU) per ml[36] for wild-type *Msmeg*,
134 and compared this to the MICs of high-density cultures (3E8 CFU/ml) under fully aerated
135 conditions. As expected, the MIC and MBC for both combinations were significantly elevated at
136 high bacterial densities, however, both antibiotic combinations retained sufficient potency to
137 reduce the bacterial population >1000-fold within 72h (Figure S1A; Figure 1A). We then evaluated
138 both spontaneous and stress-induced persister cell formation under these conditions in *Msmeg*.
139 We compared logarithmically growing (mid-log) cultures in rich 7H9 media to cultures starved for
140 2 days in PBS prior to antibiotic exposure. Consistent with expectations, we found a marked
141 increase in the frequency of persister cells in starved cultures, with a 100-fold increase in survival
142 following TIG/LZD exposure and a 10,000-fold increase following RIF/INH/EMB exposure.
143
144 We next examined two additional species of pathogenic mycobacteria to assess starvation-
145 induced persister formation under these high-density conditions. Prior work demonstrated that
146 multiple stresses, including starvation, induces persister cell formation in both *Mtb* and *Mabs*[37,38,
147 39,40]. We again compared cells starved in PBS to mid-log cells growing 7H9, and again found that
148 cultures of wild-type *Mabs* (ATCC 19977 strain) and *Mtb* (Erdman) also displayed dramatic
149 increases in the frequency of persister cells in nutrient-deprived cultures (Figure 1B,C). Notably,
150 for *Mabs* and *Msmeg,* the development of these persister cells required an adaptation period of
151 several days in nutrient-limited conditions, as formation of persister cells was dramatically
152 impaired if cells were shifted immediately into starvation conditions with antibiotics, suggesting a

153 regulated process needed to be completed, and persister cells were not simply slow growing cells
154 (Figure S2).
155
156 **Identification of pathways needed for persister formation in *Mabs***
157 We next used these conditions to carry out a Tn-Seq screen in *Mabs* to identify genes necessary
158 for forming both spontaneous and starvation-induced persister cells in response to clinically-
159 relevant antibiotics (TIG/LZD). We conducted the screen using a *Mabs Himar1* Tn library library[29]
160 comprised of ~55,000 mutations across all 4,992 non-essential *Mabs* genes in strain 19977. We
161 maintained cells in log-phase growth in 7H9 rich media, or starved cells in PBS as described
162 above, and then exposed them to TIG/LZD for 6 days, a point at which spontaneous persister
163 cells comprise the majority of the population and there is minimal further loss in viability of
164 antibiotic treated mid-log cultures (Figure 1C). Following antibiotic exposure cells were then
165 washed and placed in antibiotic-free liquid media to recover, genomic DNA was isolated, and Tn
166 insertion sites sequenced. We then used TRANSIT software[41] to quantify the abundance of each
167 Tn mutant across different conditions and identify mutants with statistically-significant differences
168 in distribution in order to identify mutations altering the ability of *Mabs* to form persister cells
169 (Figure 2A). We identified 277 *Mabs* genes required for surviving TIG/LZD exposure in rich media,
170 271 genes required for survival during starvation and 362 genes required to survive the combined
171 exposure to antibiotics and starvation (FDR < 0.05, Log2 fold-change >0.5; Figure 2B-E). Of the
172 genes required for persister survival, roughly 60% were required in both nutrient-replete and
173 starvation states, although condition-specific survival determinants were also seen (Figure 2F).
174 We identified several discrete pathways involved in spontaneous persister cell formation in *Mabs*
175 when log-phase cultures in rich media were exposed to antibiotics. As expected, we identified
176 genes with already-established functions in antibiotic responses, including MAB_0984c,
177 MAB_2752, MAB_2753 which are all homologs of known antibiotic transporters in *Mtb,* and the
178 tetracycline-responsive transcription factors MAB_4687 and MAB_0314c (Table S1).

179 Identification of multiple genes known to be involved in bacterial responses to antibiotic
180 demonstrates an ability of Tn-Seq to identify physiologically relevant pathways in this context.
181
182 Interestingly, although cells were exposed to translation-inhibiting antibiotics, and no exogenous
183 oxidative or nitrosative stress was applied to the cells, we identified a number of factors needed
184 to combat these stresses and their consequences. This includes *bfrB* (bactoferritin), *aphe*
185 (peroxiredoxin) and *katG* (catalase/peroxidase) as well as 5 components of the bacterial
186 proteasome pathway, known to mediate survival in *Mtb* during nitrosative stress. We also
187 identified members of DNA-damage response pathways including *recF* and *recG* and *uvrA*, *uvrB*
188 and *uvrC* (Figure 2G). Examining starvation-induced persisters, a number of the same pathways
189 were again seen. The mutant with the greatest persister defect in this context was *mntH*, a redox-
190 regulated Mn/Zn transporter implicated in peroxide resistance in other organisms[42, 43] (Table S1).
191 Taken together, these findings suggest an unexpected scenario whereby translation inhibition
192 triggers accumulation of reactive oxygen or nitrogen species and damage to macromolecules
193 such as DNA was occurring.
194
195 We next sought to independently confirm the role in antibiotic persistence for a set of genes
196 identified in the Tn-Seq screen. We selected a set of high-priority genes with strong defects in
197 persister formation and used oligonucleotide-mediated recombineering (ORBIT)[44] to disrupt their
198 open reading frames. The initial genes we selected were *pafA* (proteasome pathway), *katG*
199 (catalase/peroxidase), *recR* (DNA repair), *blaR* (β-lactam sensing), and *MAB1456c*
200 (cobalamin synthesis). To control for non-specific effects of antibiotic selection during the
201 recombineering process, we used the same methods to create a parallel strain targeting a non-
202 coding intergenic region downstream of a redundant tRNA gene (MAB_t5030c). We then
203 individually screened each of these mutants to determine if they displayed deficits in persister cell

204 formation. We exposed cells to TIG/LZD, either in rich 7H9 media or under starvation conditions,
205 as had been done in the as in the pooled Tn-Seq screen. For Δ*katG* we detected clear defects in
206 persister cell formation following 6 days of antibiotic exposure in either starved or starvation-
207 induced conditions, and for Δ*pafA* there was a trend toward impairment under starved conditions
208 (Figure 3A,B).
209
210 To confirm the role of *katG* and *pafA* and exclude off-target or polar effects, we performed genetic
211 complementation analysis by restoring a wild-type copy of each gene into the respective Δ*pafA*
212 and Δ*katG* mutants. In each case, we integrated a single copy of the wild-type gene, under the
213 control of its endogenous promoter, into the genome at the L5 *attB* site (hereafter *pafA*+*, katG*+
214 strains), and constructed isogenic control strains with empty vector integrated at the same site
215 (hereafter *pafA*-*, katG*- strains). We confirmed expression of the re-introduced copy of each gene
216 by RT-qPCR in the *pafA*+, and *katG*+ strains, and found expression within roughly 2-fold of
217 endogenous wild-type levels (Figure 4A,B). In rich media, the *katG*+ strain had a significant, albeit
218 incomplete restoration of persister survival, with a roughly 50-fold increase relative to the *katG*-
219 strain following antibiotic exposure. When exposed to antibiotics under starvation conditions,
220 where the *katG*- defect is more severe, the *katG*+ strain showed a near-complete restoration of
221 survival relative to control cells and over 1000-fold greater than *pafA*- cells (Figure 4C). Analysis
222 of *pafA* mutants also showed restoration of survival in *pafA*+ cells relative to *pafA*- cells although
223 the overall magnitude of the defect in *pafA*- cells was smaller than in *katG*- cells. We next
224 evaluated whether the *pafA*-, and *katG*- strains were overall more sensitive to the growth inhibitory
225 effects of TIG/LZD, or whether they had more specific defects in survival. We performed MIC
226 determination for TIG and LZD individually for each strain, comparing the *katG*+/*katG*- and
227 *pafA*+/*pafA*- strains. We found that that the MICs for each of these strains were unchanged,
228 demonstrating that these mutants were not more readily inhibited by these antibiotics. Instead,

229 they have more rapid kinetics of cell death at concentrations above the MIC, consistent with a
230 specific defect in persister cell formation or survival (Figure 4A,B).
231
232 **Reactive oxygen contributes to antibiotic lethality in *Mabs***
233 We next investigated the role of KatG in persister cell formation more broadly. We assessed
234 whether *katG* conferred protection from other antibiotics with diverse mechanisms of action, and
235 evaluated a panel of antibiotics are used to treat mycobacterial infections. Because *katG*- mutants
236 showed the greatest defects in starvation-induced persistence, we analyzed survival of *katG*+ and
237 *katG*- strains in starvation-adapted cultures and challenged cells with a panel of antibiotics.
238 Because both TIG and LZD both act by inhibiting translation, we began by exposing cells to either
239 TIG or LZD alone. As expected, the degree of bacterial killing was significantly less with either
240 agent alone than when they are added in combination. Upon exposure to either of these antibiotics
241 the *katG*- cells died more rapidly than *katG*+ cells, though we note that the final proportion of
242 persisters in the population was unchanged in *katG*- cells (Figure 5A). When we exposed cells to
243 rifabutin (RFB), an RNA polymerase inhibitor, we saw a similar effect, with a 100-fold loss of
244 viability in *katG*- cells relative to the *katG*+ cells. In contrast, when we exposed cultures to either
245 levofloxacin (gyrase inhibitor) or cefoxitin (β-lactam inhibitor of peptidoglycan cross-linking), *katG*
246 had little to no effect on cell viability (Figure 5A). Thus, the role of KatG is context-dependent
247 suggesting that some antibiotics generate oxidative stress that can be ameliorated by KatG
248 catalase/peroxidase activity while others do not.
249
250 We next assessed whether ROS is playing a role in antibiotic-mediated cell-death in *Mabs*. The
251 identification of *katG* as essential for persister cells to survive exposure to TIG/LZD, suggests that
252 ROS are present and leading to toxicity. Although TIG/LIN are translation inhibitors that do not
253 directly generate ROS we evaluated whether they might nonetheless be triggering ROS
254 accumulation as a secondary effect, and if the decreased survivability of *katG* mutants might be

255 attributable to ROS. We began by examining ROS levels in *katG+ Mabs* using the ROS indicator
256 dye cellROX, that is retained in cells when it becomes oxidized[45]. At baseline, during log-phase
257 growth in rich media < 3% of cells had ROS accumulation (Figure 5B). We saw a modest increase
258 in ROS accumulation in starved cultures, with roughly 10% of the population cellROX+. However,
259 when starved cultures were exposed to the TIG/LZD we saw a dramatic increase in ROS
260 accumulation with over 30% cellROX+ cells. Taken together, these data indicate that translation
261 inhibition does indeed have unanticipated downstream effects on cellular redox balance, with
262 ROS accumulation that could be contributing to cell death.
263
264 We next sought to test whether ROS were contributing to bacterial cell death by reducing their
265 generation and assessing the impact on cell survival. Under normal aerobic conditions, a major
266 source of ROS is oxidative phosphorylation, as superoxide, hydrogen peroxide, and hydroxyl
267 radicals are natural byproducts of the reduction of O_2 to H_2O. We tested the hypothesis that
268 oxidative phosphorylation is the source of ROS in antibiotic-treated cells by shifting cultures to
269 hypoxia, in order to block cellular respiration and associated ROS generation. A well-established
270 system for studying hypoxia in mycobacteria is the Wayne Model of gradual-onset hypoxia
271 whereby low-density cultures are inoculated in sealed vessels with minimal headspace. As the
272 culture slowly grows, the soluble O_2 in the culture is consumed, resulting in a slow onset of hypoxia
273 over several days, a process that can be monitored by the decolorization of Methylene Blue dye
274 in the media[46]. Under aerobic conditions in rich media, we observed the expected rapid killing of
275 *Mabs* over the first 5 days with the combination of TIG/LZD, with more rapid loss of viability in
276 KatG- cells (Figure 5C). However under hypoxic conditions, where oxidative phosphorylation is
277 blocked and ROS production suppressed we saw much slower bacterial killing. Importantly, under
278 hypoxic conditions *katG-* cells were no longer defective in persister formation relative to *katG+*
279 cells, consistent with the hypothesis that translation-inhibiting antibiotics also cause secondary
280 accumulation of lethal ROS in antibiotic treated cells.

281

282 We next tested the role of KatG in *Mabs* clinical strains to determine how prevalent the role of
283 *katG* in persister formation is amongst different *Mabs* strains. We obtained 2 clinical strains of
284 *Mabs*, and used ORBIT to target the *katG* locus, and again targeted the tRNA-proximal intergenic
285 site as a negative control. We then evaluated the ability of these strains to form both spontaneous
286 and starvation-induced persister cells upon exposure to TIG/LZD. For clinical strain 1, the Δ*katG*
287 mutant showed no defects in either spontaneous or stress-induced persister cell formation (Figure
288 6B). In contrast, for clinical strain 2, *katG* contributed to starvation-induced persistence, as Δ*katG*
289 displayed dramatic defects in survival (Figure 6C). Interestingly, this phenotype only manifest
290 during starvation, and was not seen in the absence of stress. Thus, loss of *katG* displays
291 incomplete penetrance, and the degree of protection conferred by KatG falls along a continuum
292 among *Mabs* strains, with strains showing no impairment in Δ*katG* cells, some showing defects
293 in both spontaneous and stress-induced persister survival, and some showing context-dependent
294 defects. Taken together these results show that antibiotics do trigger ROS accumulation in *Mabs*,
295 and that detoxification factors like KatG contribute to persister cell survival.

296

297

298 **DISCUSSION:**

299 **Pathways necessary for persister formation in Mabs.** The phenomenon of bacterial persister
300 cell formation has been recognized since the 1940s, and has been observed in a broad array of
301 bacterial species. Despite this, a unifying mechanism of persister cell formation has not emerged,
302 suggesting that different pathways may play a role in different contexts. A large body of work
303 comes from *E. coli* where toxin-antitoxin systems such as HipBA[15], Lon protease[16, 47] and the
304 ppGpp synthase RelA all contribute to the formation of persister cells [48-51]. However, even within
305 this species other mechanisms seem to function, as RelA contributes to persister cell formation

306 following exposure to β-lactams, but not quinolones[52]. In addition, how exactly these pathways
307 promoter persister formation remains unclear. While ppGpp produced by RelA seems to act
308 through Lon protease[16], the critical substrates in this process are note unknown.
309
310 It is also unclear how mechanisms identified in one bacterial species may relate to the
311 mechanisms in other species. *RelA* plays a role in diverse species of bacteria, as it is essential
312 for persister cell formation in *Pseudomonas aeruginosa*[53], *Staphylococcus aureus* [54], and *Mtb*[55]
313 [19]. However, the role of this pathway does not seem to be universal, as deletion of neither *relA*
314 nor *lon* had an effect on persister formation in *Msmeg* [56]. Conversely, other pathways have been
315 identified as critical in other organisms, including a reduction ATP synthesis in *S. aureus* [57].
316
317 In our dataset we identified a number of pathways contributing to persister cell formation following
318 exposure to translation-inhibiting antibiotics. This includes multiple members of the bacterial
319 proteasome, proteins involved in reactive oxygen and nitrogen species, and DNA repair pathways.
320 Interestingly, we did not identify *relA*, however, a prior study of the *relA Mabs* mutant demonstrates
321 that this strain still synthesizes ppGpp, suggesting possible genetic redundancy and a need to
322 disrupt one or more additional genes in a *relA* mutant background in order to study the role of
323 ppGpp synthesis in *Mabs* persister cell formation.
324
325 **Mechanisms of antibiotic lethality**
326 The mechanisms of bacterial cell death following antibiotic exposure itself remain somewhat
327 controversial. The most straightforward explanation is that antibiotics kill by directly disrupting the
328 function of their target molecule. For example, in this model cell-wall stability inhibitors lead to
329 direct mechanical lysis, and translation inhibitors act by depleting one or more essential proteins
330 below a critical threshold[21,22,58]. However, more recently it was postulated that antibiotics kill
331 through a final common pathway of lethal ROS generation, leading to oxidative damage to DNA

332 and other macromolecules[59]. Since that time, there have been studies both supporting[19,10,20] and
333 refuting the role of ROS[21, 22] in antibiotic-mediated cell death in a variety of organisms.
334
335 Our analysis of *Mabs* provides new insights into the role of ROS in antibiotic mediated killing.
336 Consistent with a role for ROS generation contributing to lethality, we find elevated ROS levels in
337 bacteria exposed to translation inhibitors. In addition, using Tn-Seq, we identified the *katG*
338 catalase/peroxidase gene as contributing to persister cell viability in both log-phase and nutrient-
339 starved cells. When oxygen is removed from the cultures, not only is antibiotic killing slowed, but
340 importantly, the *katG* mutant no longer displays a survival defect. Taken together, these data
341 demonstrate that in *Mabs*, translation inhibitors such as TIG or LIN do indeed have an indirect
342 downstream effect triggering ROS accumulation, and that KatG-mediated detoxification of these
343 ROS is important for survival. These findings are supported by other published studies. In *Mabs*
344 other groups have also observed reduced antibiotic-mediated killing in hypoxic conditions[37]. In
345 *Mtb*, exposure to rifampin also generates ROS[19, 60], and *katG* is found in Tn-Seq datasets
346 examining rifampin-treated cells[19].
347
348 The source of ROS in this setting is uncertain. In principle, any of several derangements could
349 lead to ROS accumulation. One of the major sources of cellular ROS is oxidative phosphorylation,
350 as hydrogen peroxide, superoxide, and hydroxyl radicals are natural byproducts of the reduction
351 of O_2 to H_2O by the electron transport chain. Thus, increased ROS generation by the electron
352 transport chain is an attractive hypothesis. Alternatively, particularly under starvation conditions,
353 it is possible that antioxidant and ROS scavenging metabolites may become depleted, thus
354 accelerating oxidative damage. Our Tn-Seq analysis provides additional insight on this. We noted
355 a small class of Tn mutants that were better able to survive antibiotic exposure (Figure 2B).
356 Prominent among this class of mutants were several independent components of the NADH
357 dehydrogenase complex. Also known as Complex I of the electron transport chain, this complex

358 is one of the entry points for electrons into the oxidative phosphorylation pathway. The observation
359 that mutants in this complex are protected suggests that decreasing flux through oxidative
360 phosphorylation, with a concomitant decrease in ROS generation, may enhance survival during
361 antibiotic exposure.
362
363 However, antibiotic-induced ROS accumulation is not a universal phenomenon. Other antibiotics
364 we examined in *Mabs* do not trigger ROS accumulation, and loss of *katG* had no effect on survival
365 in these antibiotics. In addition, ROS detoxification does not always play a protective role, as loss
366 of catalase and peroxidase activities in E. coli had no effect on persister survival[22]. Taken together,
367 this suggests a model in which antibiotics cause direct toxicity by acting on their target, but in
368 addition some antibiotics, notably transcription inhibitors and translation inhibitors, also appear to
369 have a secondary toxic effect of causing ROS accumulation. How exactly transcription or
370 translation blockade lead to increased ROS levels is currently unclear and will require further
371 investigation, although our data suggest that the electron transport chain plays an important role.
372
373 **Therapeutic implications**
374 *Mabs* infections are particularly challenging to eradicate, with relapse rates over 50%[28]. Our
375 results highlight several bacterial processes such as the bacterial proteasome or ROS
376 detoxification that might targeted therapeutically to reduce the development or survival of persister
377 cells. Agents targeting these process might not have any antimicrobial activity alone, but might
378 act to target the unique physiology of persister cells that develop upon antibiotic exposure. This
379 would represent a new therapeutic class of “persistence inhibitors” that might act cooperatively
380 with traditional antibiotics to eliminate the subpopulation of persister cells that would otherwise
381 survive prolonged antibiotic exposure.
382
383 **Limitations**

384 Tn-Seq screens have inherent drawbacks, including an inability to identify mutants in essential
385 genes, or in cases of genetic redundancy. Thus, there are likely genes needed for spontaneous
386 or starvation-induced persister cell formation in *Mabs* that were not identified in this study. In
387 addition, we studied a exposure to a single class of antibiotic, focusing on the translation inhibitors
388 often used to treat *Mabs* infections, and we studied only spontaneous and starvation-induced
389 persister cells. It is likely that studying other antibiotics, with different mechanisms of action, or
390 different stresses that induce persister cells would identify additional genes contributing to
391 persister formation and would allow better identification of pathways that might be shared
392 amongst different classes of antibiotic.
393
394
395 **MATERIALS AND METHODS**
396 Bacterial Strains and Culture conditions:
397 *Mabs* ATCC 19977 and clinical *Mabs* strains were grown in BD Middlebrook 7H9 media (liquid)
398 or 7H10 media (solid) supplemented with 0.5% glycerol (Sigma) and 0.2% Tween-80 (Sigma).
399 Sacramento Clinical strains were obtained from the Sacramento County Department of Public
400 health mycobacteriology laboratory. Identity of strains as *Mabs* was confirmed by amplification of
401 the 16s locus and Sanger sequencing. *Msmeg* (MC2 155) was grown in the same media as *Mabs*.
402 *Mtb* Erdman was grown in 7H9 (liquid) or 7H10 (solid) supplemented with 0.5% glycerol, 0.1%
403 Tween-80, and 10% OADC (BD). All cultures were grown at 37C and liquid cultures were shaken.
404 With all liquid cultures, cultures were grown with 90% container headspace or using a gas
405 permeable cap to ensure culture oxygenation. PBS starvation was achieved by washing OD0.5-
406 1.0 *Mabs* 1X in DPBS (-Ca/Mg) and resuspending in DPBS supplemented with 0.1% tyloxapol
407 (Sigma).
408
409 *Mabs* antibiotic killing experiments:

410 For PBS starvation experiments, freezer stocks of *Mabs* were thawed and grown for 48 hours in
411 log phase, then PBS starved or passaged in log phase for 48h. OD0.5-1.0 or PBS starved *Mabs*
412 were then resuspended in antibiotic containing media at OD1.0. For experiments with hypoxia,
413 *Mabs* was adjusted to OD0.001 in media with 1.5ug/ml methylene blue and added to a rubber
414 septum sealed glass vial with 50% headspace. These cultures were grown for 5d, and methylene
415 blue discoloration was observed at d3. Antibiotics were used at the following concentrations:
416 tigecycline (Chem-Impex) at 10ug/ml (8 fold above MIC, re-administered every 3 days), linezolid
417 (Chem-Impex) at 100ug/ml (20 fold above MIC), levofloxacin (Sigma) at 40ug/ml (8 fold above
418 MIC), cefoxitin (Sigma) at 80ug/ml (8 fold above MIC, re-administered every 3 days), and rifabutin
419 (Cayman) at 40ug/ml (4 fold above MIC). After antibiotic administration, colony forming units over
420 time were measured.
421
422 *Msmeg* antibiotic killing experiments:
423 Freezer stocks of *Msmeg* were streaked to agar plates, grown at 37C until colonies formed (3
424 days), then stored at room temperature for up to one additional week. Individual colonies were
425 picked and grown for 48 hours in log phase before being PBS starved or passaged in log phase
426 for 48h. OD0.5-1.0 or PBS starved *Msmeg* were then resuspended in antibiotic containing media
427 at OD1.0. Antibiotics were used at the following concentrations: tigecycline (Chem-Impex) at
428 1.25ug/ml (8 fold above MIC, re-administered every 3 days), linezolid (Chem-Impex) at 2.5ug/ml
429 (8 fold above MIC), rifampin (Sigma) at 32ug/ml (8 fold above MIC, re-administered every 6 days),
430 isoniazid (Sigma) at 32ug/ml (8 fold above MIC, re-administered every 6 days), and ethambutol
431 (Thermo) at 4ug/ml (8 fold above MIC, re-administered every 3 days). After antibiotic
432 administration, colony forming units over time were measured.
433
434 *MTB* antibiotic killing experiments:

435 Freezer stocks of *MTB* were thawed and grown for 5-7 days in log phase before being starved for
436 14d or longer. Non-starved control bugs were thawed such that they were also grown for 5-7 days
437 in log phase before experimental use. OD0.5-1.0 or PBS starved *MTB* was then resuspended in
438 antibiotic containing media and adjusted to OD1.0. Antibiotics were used at the following
439 concentrations: rifampin (Sigma) at 0.1ug/ml (4 fold above MIC, re-administered every 6 days),
440 isoniazid (Sigma) at 0.1ug/ml (4 fold above MIC, re-administered every 6 days), and ethambutol
441 (Thermo) at 8ug/ml (4 fold above MIC, re-administered every 6 days). After antibiotic
442 administration, colony forming units over time were measured.
443
444 Transposon insertion sequencing:
445 The transposon (Tn) library for Mabs was constructed as previously described for other
446 mycobacterial species[41]. Screening was done by growing a freezer stock of the library for 2.5
447 days in log phase before 48 hour PBS starvation or continued log phase growth. Samples were
448 then resuspended in tigecycline/linezolid or DMSO solvent containing media and left for 6 days
449 (with a re-administration of tigecycline or matching DMSO on day 3). The samples were then
450 washed 2X in antibiotic free liquid media and grown until OD0.5-1.0. Subsequently, the samples
451 underwent three more rounds of 100-fold passaging in liquid media before the samples were
452 collected in trizol (Invitrogen). A sample taken at the time of the commencement of PBS starvation
453 was collected in trizol and used as the input control. Three independent trials of this experiment
454 were run to achieve triplicate data. DNA was extracted and submitted to the UC Davis DNA
455 Technologies Core, where Himar1 transposon containing sequences were amplified and
456 sequenced on Illumina AVITI. Sequence reads were mapped to the ATCC 19977 genome and
457 analyzed using TRANSIT software. The resampling method was used with the following
458 parameters: 0% of N/C termini ignored, 10,000 samples, TTR normalization, LOESS correction,
459 include sites with all zeros, site restricted resampling. For follow-up analysis, adjusted p value
460 <0.05 and log2 fold change <-0.5 (essential) or >0.5 (less essential) was used a cutoff for

461 statistical significance. Mabs gene orthology to Mtb was done with BLASTp using an e-value
462 cutoff of 0.1. Mabs genes and MTB genes that mapped to each other using independent one-way
463 BLASTp searches were considered orthologs. For pathway analysis, gene lists (*MTB* orthologs)
464 were imported into the DAVID knowledgebase and pathway enrichment analysis was done for
465 biological processes with Gene Ontology and Uniprot key words as well as KEGG pathways.
466 Duplicated pathways were filtered out and the top pathways by adjusted p value were reported.
467
468 Gene Deletion and complementation:
469 Knockout strains were generated using ORBIT {Murphy, 2018 #325}. Briefly, *Mabs* was
470 transformed with the kanR ORBIT recombineering plasmid pkm444. 20ml Mab at OD0.5-1.0 was
471 washed 2X in 10% glycerol and resuspended in 200ul 10% glycerol. 500ng plasmid was added
472 and electroporated at 2.5kV in 0.2cm cuvettes. The bacteria were allowed to recover overnight
473 before plating on 150ug/ml kan plates. Clones were selected and regrown in liquid media
474 supplemented with 150ug/ml kan and 10% OADC (BD) to OD0.5-1.0. The pkm444-*Mabs* was
475 then diluted to OD0.1 and 200mM glycine (sigma) was added to the media. 16 hours later, 500mM
476 sucrose (Sigma) and 500ng/ml aTC (Cayman) were added and incubated for an additional 4
477 hours. Subsequently, the Mab was washed 2X in ice cold 10% glycerol + 500mM sucrose. 200ul
478 of 10X concentrated *Mabs* was then electroporated with 600ng of the ZeoR ORBIT payload
479 plasmid pkm496 and 2ug of targeting oligonucleotide (supplementary table 3) at 2.5kV in 0.2cm
480 cuvettes. The Mab was then allowed to recover overnight in liquid media with 10% OADC and
481 500ng/ml aTC and plated on 150ug/ml zeocin plates. Mutants were then selected and screened
482 for gene deletion by PCR amplification and confirmed by sanger sequencing. For genetic
483 complementation, knockout strains were complemented with PCR amplified WT copies of their
484 knocked-out gene. Error-free KatG and PafA PCR amplification and vector integration was
485 confirmed by sanger sequencing. At least 100bp of upstream and downstream sequence was
486 also included, allowing for retention of the endogenous promoter and terminator. Since *katG* is

487 known to be transcribed as part of an operon, the upstream gene FurA was also included in the
488 complementation construct to achieve maximal KatG expression. The mycobacterial integrating
489 vector pmv306 was used and cloning was done by SLIC. Subsequently, complementation was
490 confirmed by RNA extraction and RT-qPCR.
491
492 MIC plates
493 Two-fold serial dilutions of antibiotics were prepared in a 96 well plate in 100ul volume. 100ul of
494 2X bacteria were added (for Mab: used a final OD of 0.001, M. smegmatis: OD0.001, MTB:
495 OD0.01), making a final volume of 200ul. The plates were incubated until there was visible growth
496 in the no antibiotic control well. At this time, MICs were assessed visually, and the bacteria were
497 transferred to a new plate with 20ul of 40% PFA. OD620 measurements were taken in a FilterMax
498 F3 plate reader (Molecular Devices).
499
500 Flow cytometry
501 OD1 Mab was stained with cellROX green (Thermo) at a final concentration of 5mM for 30min at
502 37C. The cells were then washed in PBS and resuspended in PBS with 4% PFA and 5ug/ml DAPI.
503 The samples were run on a LSRII flow cytometer (BD) and analyzed with FlowJo software (BD).
504
505 **FIGURE LEGENDS**

506 **Figure 1. Nutrient starvation induces antibiotic persister cell formation across**
507 **mycobacteria.** (A) *M. smegmatis* (MC^2 155), (B) *M. tuberculosis* (Erdman), or (C) *M. abscessus*
508 (ATCC 19977) were starved in PBS or grown in 7H9 rich media. The indicated antibiotics were
509 added: Isoniazid (INH), rifampin (RIF), ethambutol (EMB) tigecycline (TIG) and linezolid (LZD).
510 Surviving colony forming units (CFUs) are shown. Error bars represent SEM, statistical

511 significance is calculated at each time point using student's t test. ****: p<0.0001, ***: p<0.001,
512 **: p<0.01, *: p<0.05, ns: p>0.05. Data are combined from 3 independent experiments.

513 **Figure 2. *Mabs* Tn-seq identifies genes essential for persister cell survival.** (A)
514 Experimental design (B-E) Relative abundance of individual genes under the indicted conditions
515 using Tn-Seq. For B-D comparisons are made to the input log-phase population. The additional
516 comparison in E is made to PBS starvation. When antibiotics are not added an equal amount of
517 DMSO solvent is added. Cultures were fully aerated. (F) Distribution of genes essential for each
518 indicated condition relative to the input population (FDR < 0.05, Log2 fold-change >0.5). (G)
519 Pathway analysis of the essential genes in each condition, showing significantly enriched
520 pathways using the NIH DAVID knowledgebase. Screens were run as 3 independent
521 experiments and data is from the combined results.

522 **Figure 3. Independent gene deletions of *katG* and *pafA* confirm Tn-Seq results.** Survival
523 over time for the indicated genes following exposure to TIG/LZD either in 7H9 rich media or
524 following starvation for 48h in PBS. ORBIT recombineering mutants were made in ATCC 19977
525 to disrupt (A) *katG* (Catalase-peroxidase), (B) *pafA* (Pup protein ligase), (C) *MAB1456c/cobA*
526 (cobalamin synthesis), *blaR* (β-lactam sensing), *recR* (Recombination protein RecR). A-B are
527 combined data from 4 independent experiments. C-E is representative data from 2 independent
528 experiments. Error bars represent SEM, statistical significance is calculated at each time point
529 using student's t test. ****: p<0.0001, ***: p<0.001, **: p<0.01, *: p<0.05, ns: p>0.05.

530 **Figure 4. Complementation analysis *katG* and *pafA* mutants confirms their role in**
531 **persister survival.** Analysis of *katG- (ΔkatG::pmv306), katG+ (ΔkatG::pmv306 katG), pafA-*
532 *(ΔpafA::pmv306), pafA+ (pafA::pmv306 pafA)*and control strain (intergenic
533 site*::zeoR::pmv306).* MIC determination for (A) *katG+/katG-* and (B) *pafA+/pafA-* strains.
534 Survival over time for (C) *katG+/katG-* and (D) *pafA+/pafA-* strains. Error bars represent
535 standard deviation, mean expression is displayed above the bar for each group, data are 3

536 technical replicates from one experiment. ****: p<0.0001, ***: p<0.001, **: p<0.01, *: p<0.05, ns:
537 p>0.05.

538 **Figure 5. Context-specific accumulation of ROS and role for *katG*.** (A) Analysis of
539 *katG+/katG-* cells when challenged with a panel of antibiotics. Cells were starved in PBS for 48h
540 to induce persister cells and then exposed to the indicated antibiotic at 4x MIC. (B) Flow
541 cytometry of DAPI and cellROX stained *katG*$^{+}$ *Mabs* after 72h in each condition are shown.
542 Percentage of cells in the cellROX+ gate are shown for each plot. (C) Persister survival over
543 time for aerated and hypoxic and cultures of *Mabs* comparing *katG+/katG-* cells after treatment
544 with TIG/LIN are shown. Statistical significance is calculated between antibiotic treated
545 *katG+/katG-* cells *Mabs.* Error bars represent SEM, statistical significance is calculated at each
546 time point using student's t test. ****: p<0.0001, ***: p<0.001, **: p<0.01, *: p<0.05, ns: p>0.05.

547 **Figure 6. Variable penetrance of *katG* phenotype among *Mabs* strains** Δ*katG* and control
548 strains were generated in the indicated strain backgrounds using ORBIT recombineering: (A)
549 ATCC 19977, (B) Sacramento County clinical strain #1 and (C) clinical strain #2. Error bars
550 represent SEM, statistical significance is calculated at each time point using student's t test.
551 ****: p<0.0001, ***: p<0.001, **: p<0.01, *: p<0.05, ns: p>0.05.

552

553 **Figure S1. Antibiotic concentration and culture density.** (A-E) *Msmeg* was grown to log
554 phase, concentration adjusted to either 3e7 cells/ml or 5e5 cells/ml, and treated with antibiotics
555 across the indicated range of concentrations. OD measurements after 36 hours of growth are
556 shown for (A) Tigecycline, (B) Linezolid, (C) Isoniazid, (D) Rifampin, and (E) Ethambutol. The
557 antibiotic concentrations used in subsequent experiments are labelled with an arrow.

558

559 **Figure S2. Adaption to starvation prior to antibiotic administration is required for**
560 **persister cell induction**. (A) *Msmeg,* (B) *Mtb*, or (C) *Mabs* were starved in PBS or grown in
561 7H9 rich media. At day 0, all the indicated cultures were changed to PBS with antibiotics and kill
562 kinetics are shown. Antibiotics in nutrient rich media are included as a control. Error bars
563 represent SEM, statistical significance was calculated between PBS+abx conditions at each
564 time point using student's t test. ****: $p<0.0001$, ***: $p<0.001$, **: $p<0.01$, *: $p<0.05$, ns: $p>0.05$.
565 All graphs are combined from 3 independent experiments.

566

567 **Table S1. Tn-Seq results**

568 **Table S2. DAVID functional pathway analysis**

569 **Table S3. Oligonucleotide sequences**

570

571

572 **REFERENCES**

573 1. Stevens, D.L., A.L. Bisno, H.F. Chambers, E.P. Dellinger, E.J. Goldstein, S.L. Gorbach,
574 J.V. Hirschmann, S.L. Kaplan, J.G. Montoya, and J.C. Wade, *Practice guidelines for the*
575 *diagnosis and management of skin and soft tissue infections: 2014 update by the*
576 *Infectious Diseases Society of America.* Clin Infect Dis, 2014. **59**(2): p. e10-52.
577 2. Metersky, M.L. and A.C. Kalil, *Management of ventilator-associated pneumonia:*
578 *guidelines.* Clinics in chest medicine, 2018. **39**(4): p. 797-808.
579 3. Meylan, S., I.W. Andrews, and J.J. Collins, *Targeting Antibiotic Tolerance, Pathogen by*
580 *Pathogen.* Cell, 2018. **172**(6): p. 1228-1238.
581 4. Namugenyi, S.B., A.M. Aagesen, S.R. Elliott, and A.D. Tischler, *Mycobacterium*
582 *tuberculosis PhoY Proteins Promote Persister Formation by Mediating Pst/SenX3-*
583 *RegX3 Phosphate Sensing.* mBio, 2017. **8**(4): p. e00494-17.
584 5. Liu, Y., S. Tan, L. Huang, R.B. Abramovitch, K.H. Rohde, M.D. Zimmerman, C. Chen, V.
585 Dartois, B.C. VanderVen, and D.G. Russell, *Immune activation of the host cell induces*
586 *drug tolerance in Mycobacterium tuberculosis both in vitro and in vivo.* Journal of
587 Experimental Medicine, 2016. **213**(5): p. 809-825.
588 6. Gold, B. and C. Nathan, *Targeting Phenotypically Tolerant Mycobacterium tuberculosis.*
589 Microbiol Spectr, 2017. **5**(1).
590 7. Bigger, J.J.T.L., *Treatment of staphylococcal infections with penicillin by intermittent*
591 *sterilisation.* 1944. **244**(6320): p. 497-500.
592 8. Ronneau, S., P.W.S. Hill, and S. Helaine, *Antibiotic persistence and tolerance: not just*
593 *one and the same.* Current opinion in microbiology, 2021. **64**: p. 76-81.
594 9. Dhar, N. and J.D. McKinney, *Microbial phenotypic heterogeneity and antibiotic tolerance.*
595 Current opinion in microbiology, 2007. **10**(1): p. 30-38.

596 10. Grant, S.S., B.B. Kaufmann, N.S. Chand, N. Haseley, and D.T. Hung, *Eradication of*
597 *bacterial persisters with antibiotic-generated hydroxyl radicals.* Proceedings of the
598 National Academy of Sciences, 2012. **109**(30): p. 12147-12152.
599 11. Baker, J.J. and R.B. Abramovitch, *Genetic and metabolic regulation of Mycobacterium*
600 *tuberculosis acid growth arrest.* Scientific Reports, 2018. **8**(1).
601 12. Saito, K., T. Warrier, S. Somersan-Karakaya, L. Kaminski, J. Mi, X. Jiang, S. Park, K.
602 Shigyo, B. Gold, and J. Roberts, *Rifamycin action on RNA polymerase in antibiotic-*
603 *tolerant Mycobacterium tuberculosis results in differentially detectable populations.*
604 Proceedings of the National Academy of Sciences, 2017. **114**(24): p. E4832-E4840.
605 13. Hipolito, V.E.B., E. Ospina-Escobar, and R.J. Botelho, *Lysosome remodelling and*
606 *adaptation during phagocyte activation.* Cell Microbiol, 2018. **20**(4).
607 14. Sukumar, N., S. Tan, B.B. Aldridge, and D.G. Russell, *Exploitation of Mycobacterium*
608 *tuberculosis reporter strains to probe the impact of vaccination at sites of infection.* PLoS
609 Pathog, 2014. **10**(9): p. e1004394.
610 15. Schumacher, M.A., K.M. Piro, W. Xu, S. Hansen, K. Lewis, and R.G. Brennan, *Molecular*
611 *Mechanisms of HipA-Mediated Multidrug Tolerance and Its Neutralization by HipB.*
612 Science, 2009. **323**(5912): p. 396-401.
613 16. Harms, A., C. Fino, A. Sørensen Michael, S. Semsey, and K. Gerdes, *Prophages and*
614 *Growth Dynamics Confound Experimental Results with Antibiotic-Tolerant Persister*
615 *Cells.* mBio, 2017. **8**(6): p. 10.1128/mbio.01964-17.
616 17. Korch, S.B., T.A. Henderson, and T.M. Hill, *Characterization of the hipA7 allele of*
617 *Escherichia coli and evidence that high persistence is governed by (p)ppGpp synthesis.*
618 Mol Microbiol, 2003. **50**(4): p. 1199-213.
619 18. Wong, F., S. Wilson, R. Helbig, S. Hegde, O. Aftenieva, H. Zheng, C. Liu, T. Pilizota, E.C.
620 Garner, A. Amir, and L.D. Renner, *Understanding Beta-Lactam-Induced Lysis at the*
621 *Single-Cell Level.* Frontiers in Microbiology, 2021. **12**.

622 19. Saito, K., S. Mishra, T. Warrier, N. Cicchetti, J. Mi, E. Weber, X. Jiang, J. Roberts, A.
623 Gouzy, E. Kaplan, C.D. Brown, B. Gold, and C. Nathan, *Oxidative damage and delayed*
624 *replication allow viable Mycobacterium tuberculosis to go undetected.* Sci Transl Med,
625 2021. **13**(621): p. eabg2612.
626 20. Vilchèze, C., T. Hartman, B. Weinrick, P. Jain, T.R. Weisbrod, L.W. Leung, J.S.
627 Freundlich, and W.R. Jacobs, Jr., *Enhanced respiration prevents drug tolerance and*
628 *drug resistance in Mycobacterium tuberculosis.* Proc Natl Acad Sci U S A, 2017. **114**(17):
629 p. 4495-4500.
630 21. Keren, I., S. Minami, E. Rubin, and K. Lewis, *Characterization and transcriptome*
631 *analysis of Mycobacterium tuberculosis persisters.* mBio, 2011. **2**(3): p. e00100-11.
632 22. Liu, Y. and J.A. Imlay, *Cell death from antibiotics without the involvement of reactive*
633 *oxygen species.* Science, 2013. **339**(6124): p. 1210-3.
634 23. de Keijzer, J., A. Mulder, J. de Beer, A.H. de Ru, P.A. van Veelen, and D. van Soolingen,
635 *Mechanisms of Phenotypic Rifampicin Tolerance in Mycobacterium tuberculosis Beijing*
636 *Genotype Strain B0/W148 Revealed by Proteomics.* J Proteome Res, 2016. **15**(4): p.
637 1194-204.
638 24. Gold, B., T. Warrier, and C. Nathan, *A multi-stress model for high throughput screening*
639 *against non-replicating Mycobacterium tuberculosis.* Mycobacteria protocols, 2015: p.
640 293-315.
641 25. Dorman, S.E., P. Nahid, E.V. Kurbatova, P.P. Phillips, K. Bryant, K.E. Dooley, M. Engle,
642 S.V. Goldberg, H.T. Phan, and J. Hakim, *Four-month rifapentine regimens with or without*
643 *moxifloxacin for tuberculosis.* New England Journal of Medicine, 2021. **384**(18): p. 1705-
644 1718.
645 26. Nahid, P., S.E. Dorman, N. Alipanah, P.M. Barry, J.L. Brozek, A. Cattamanchi, L.H.
646 Chaisson, R.E. Chaisson, C.L. Daley, and M. Grzemska, *Official American thoracic*
647 *society/centers for disease control and prevention/infectious diseases society of America*

648 *clinical practice guidelines: treatment of drug-susceptible tuberculosis.* Clinical infectious
649 diseases, 2016. **63**(7): p. e147-e195.
650 27. Griffith, D.E., T. Aksamit, B.A. Brown-Elliott, A. Catanzaro, C. Daley, F. Gordin, S.M.
651 Holland, R. Horsburgh, G. Huitt, and M.F. Iademarco, *An official ATS/IDSA statement:*
652 *diagnosis, treatment, and prevention of nontuberculous mycobacterial diseases.*
653 American journal of respiratory and critical care medicine, 2007. **175**(4): p. 367-416.
654 28. Griffith, D.E. and C.L. Daley, *Treatment of Mycobacterium abscessus Pulmonary*
655 *Disease.* CHEST, 2022. **161**(1): p. 64-75.
656 29. Rodriguez, R., N. Campbell-Kruger, J. Gonzalez Camba, J. Berude, R. Fetterman, and
657 S. Stanley, *MarR-Dependent Transcriptional Regulation of mmpSL5 Induces*
658 *Ethionamide Resistance in Mycobacterium abscessus.* Antimicrobial Agents and
659 Chemotherapy, 2023. **67**(4): p. e01350-22.
660 30. Li, S., N.C. Poulton, J.S. Chang, Z.A. Azadian, M.A. DeJesus, N. Ruecker, M.D.
661 Zimmerman, K.A. Eckartt, B. Bosch, C.A. Engelhart, D.F. Sullivan, M. Gengenbacher,
662 V.A. Dartois, D. Schnappinger, and J.M. Rock, *CRISPRi chemical genetics and*
663 *comparative genomics identify genes mediating drug potency in Mycobacterium*
664 *tuberculosis.* Nature microbiology, 2022. **7**(6): p. 766-779.
665 31. Carey, A.F., J.M. Rock, I.V. Krieger, M.R. Chase, M. Fernandez-Suarez, S. Gagneux,
666 J.C. Sacchettini, T.R. Ioerger, and S.M. Fortune, *TnSeq of Mycobacterium tuberculosis*
667 *clinical isolates reveals strain-specific antibiotic liabilities.* PLoS pathogens, 2018. **14**(3):
668 p. e1006939.
669 32. Kreutzfeldt, K.M., R.S. Jansen, T.E. Hartman, A. Gouzy, R. Wang, I.V. Krieger, M.D.
670 Zimmerman, M. Gengenbacher, J.P. Sarathy, M. Xie, V. Dartois, J.C. Sacchettini, K.Y.
671 Rhee, D. Schnappinger, and S. Ehrt, *CinA mediates multidrug tolerance in*
672 *Mycobacterium tuberculosis.* Nat Commun, 2022. **13**(1): p. 2203.

673 33. Block, A.M., S.B. Namugenyi, N.P. Palani, A.M. Brokaw, L. Zhang, K.B. Beckman, and
674 A.D. Tischler, *Mycobacterium tuberculosis Requires the Outer Membrane Lipid*
675 *Phthiocerol Dimycocerosate for Starvation-Induced Antibiotic Tolerance.* Msystems,
676 2023. **8**(1): p. e0069922.
677 34. Bellerose, M.M., S.-H. Baek, C.-C. Huang, C.E. Moss, E.-I. Koh, M.K. Proulx, C.M.
678 Smith, R.E. Baker, J.S. Lee, S. Eum, S.J. Shin, S.-N. Cho, M. Murray, and C.M. Sassetti,
679 *Common Variants in the Glycerol Kinase Gene Reduce Tuberculosis Drug Efficacy.*
680 mBio, 2019. **10**(4): p. e00663-19.
681 35. Kumar, K., C.L. Daley, D.E. Griffith, and M.R. Loebinger, *Management of Mycobacterium*
682 *avium complex and Mycobacterium abscessus pulmonary disease: therapeutic*
683 *advances and emerging treatments.* European respiratory review, 2022. **31**(163).
684 36. Woods, G.L., B.A. Brown-Elliott, P.S. Conville, E.P. Desmond, G.S. Hall, G. Lin, G.E.
685 Pfyffer, J.C. Ridderhof, S.H. Siddiqi, R.J. Wallace, Jr., N.G. Warren, and F.G. Witebsky,
686 *CLSI Standards: Guidelines for Health Care Excellence*, in *Susceptibility Testing of*
687 *Mycobacteria, Nocardiae, and Other Aerobic Actinomycetes*. 2011, Clinical and
688 Laboratory Standards Institute

689 Copyright ©2011 Clinical and Laboratory Standards Institute.; Except as stated below,
690 any reproduction of content from a CLSI copyrighted standard, guideline, companion
691 product, or other material requires express written consent from CLSI. All rights
692 reserved. Interested parties may send permission requests to permissions@clsi.org.;
693 CLSI hereby grants permission to each individual member or purchaser to make a single
694 reproduction of this publication for use in its laboratory procedure manual at a single site.
695 To request permission to use this publication in any other manner, e-mail
696 permissions@clsi.org.: Wayne (PA).

697 37. Yam, Y.K., N. Alvarez, M.L. Go, and T. Dick, *Extreme Drug Tolerance of Mycobacterium*
698 *abscessus "Persisters".* Front Microbiol, 2020. **11**: p. 359.
699 38. Berube, B.J., L. Castro, D. Russell, Y. Ovechkina, and T. Parish, *Novel Screen to Assess*
700 *Bactericidal Activity of Compounds Against Non-replicating Mycobacterium abscessus.*
701 Front Microbiol, 2018. **9**: p. 2417.
702 39. Lee, J., N. Ammerman, A. Agarwal, M. Naji, S.Y. Li, and E. Nuermberger, *Differential In*
703 *Vitro Activities of Individual Drugs and Bedaquiline-Rifabutin Combinations against*
704 *Actively Multiplying and Nutrient-Starved Mycobacterium abscessus.* Antimicrob Agents
705 Chemother, 2021. **65**(2).
706 40. Betts, J.C., P.T. Lukey, L.C. Robb, R.A. McAdam, and K. Duncan, *Evaluation of a*
707 *nutrient starvation model of Mycobacterium tuberculosis persistence by gene and protein*
708 *expression profiling.* Molecular Microbiology, 2002. **43**(3): p. 717-731.
709 41. DeJesus, M.A., C. Ambadipudi, R. Baker, C. Sassetti, and T.R. Ioerger, *TRANSIT-a*
710 *software tool for Himar1 TnSeq analysis.* PLoS computational biology, 2015. **11**(10): p.
711 e1004401.
712 42. Shi, H., R. Zhang, L. Lan, Z. Chen, and J. Kan, *Zinc mediates resuscitation of lactic acid-*
713 *injured Escherichia coli by relieving oxidative stress.* Journal of Applied Microbiology,
714 2019. **127**(6): p. 1741-1750.
715 43. Hohle, T.H. and M.R. O'Brian, *The mntH gene encodes the major Mn(2+) transporter in*
716 *Bradyrhizobium japonicum and is regulated by manganese via the Fur protein.* Mol
717 Microbiol, 2009. **72**(2): p. 399-409.
718 44. Murphy, K.C., S.J. Nelson, S. Nambi, K. Papavinasasundaram, C.E. Baer, and C.M.
719 Sassetti, *ORBIT: a new paradigm for genetic engineering of mycobacterial*
720 *chromosomes.* mBio, 2018. **9**(6): p. e01467-18.
721 45. McBee, M.E., Y.H. Chionh, M.L. Sharaf, P. Ho, M.W.L. Cai, and P.C. Dedon, *Production*
722 *of superoxide in bacteria is stress- and cell state-dependent: A gating-optimized flow*

723 *cytometry method that minimizes ROS measurement artifacts with fluorescent dyes.*
724 Frontiers in Microbiology, 2017. **8**(MAR).
725 46. Wayne, L.G. and L.G. Hayes, *An In Vitro Model for Sequential Study of Shiftdown of*
726 *Mycobacterium tuberculosis through Two Stages of Nonreplicating Persistence.* Infection
727 and Immunity, 1996. **64**(6): p. 2062-2069.
728 47. Brazas Michelle, D., B.M. Breidenstein Elena, J. Overhage, and E.W. Hancock Robert,
729 *Role of Lon, an ATP-Dependent Protease Homolog, in Resistance of Pseudomonas*
730 *aeruginosa to Ciprofloxacin.* Antimicrobial Agents and Chemotherapy, 2007. **51**(12): p.
731 4276-4283.
732 48. Kusser, W. and E.E. Ishiguro, *Involvement of the relA gene in the autolysis of*
733 *Escherichia coli induced by inhibitors of peptidoglycan biosynthesis.* Journal of
734 Bacteriology, 1985. **164**(2): p. 861-865.
735 49. Bokinsky, G., E.E.K. Baidoo, S. Akella, H. Burd, D. Weaver, J. Alonso-Gutierrez, H.
736 García-Martín, T.S. Lee, and J.D. Keasling, *HipA-Triggered Growth Arrest and β-Lactam*
737 *Tolerance in Escherichia coli Are Mediated by RelA-Dependent ppGpp Synthesis.*
738 Journal of Bacteriology, 2013. **195**(14): p. 3173-3182.
739 50. Honsa, E.S., V.S. Cooper, M.N. Mhaissen, M. Frank, J. Shaker, A. Iverson, J. Rubnitz,
740 R.T. Hayden, R.E. Lee, C.O. Rock, E.I. Tuomanen, J. Wolf, and J.W. Rosch, *RelA*
741 *Mutant Enterococcus faecium with Multiantibiotic Tolerance Arising in an*
742 *Immunocompromised Host.* mBio, 2017. **8**(1): p. e02124-16.
743 51. Nguyen, D., A. Joshi-Datar, F. Lepine, E. Bauerle, O. Olakanmi, K. Beer, G. McKay, R.
744 Siehnel, J. Schafhauser, Y. Wang, B.E. Britigan, and P.K. Singh, *Active starvation*
745 *responses mediate antibiotic tolerance in biofilms and nutrient-limited bacteria.* Science,
746 2011. **334**(6058): p. 982-6.
747 52. Kudrin, P., V. Varik, S.R.A. Oliveira, J. Beljantseva, T.D.P. Santos, I. Dzhygyr, D. Rejman,
748 F. Cava, T. Tenson, and V. Hauryliuk, *Subinhibitory Concentrations of Bacteriostatic*

Antibiotics Induce relA-Dependent and relA-Independent Tolerance to β-Lactams. Antimicrobial Agents and Chemotherapy, 2017. **61**(4): p. 10.1128/aac.02173-16.

53. Viducic, D., T. Ono, K. Murakami, H. Susilowati, S. Kayama, K. Hirota, and Y. Miyake, *Functional analysis of spoT, relA and dksA genes on quinolone tolerance in Pseudomonas aeruginosa under nongrowing condition.* Microbiol Immunol, 2006. **50**(4): p. 349-57.

54. Geiger, T., B. Kästle, F.L. Gratani, C. Goerke, and C. Wolz, *Two small (p)ppGpp synthases in Staphylococcus aureus mediate tolerance against cell envelope stress conditions.* J Bacteriol, 2014. **196**(4): p. 894-902.

55. Dutta, N.K., L.G. Klinkenberg, M.J. Vazquez, D. Segura-Carro, G. Colmenarejo, F. Ramon, B. Rodriguez-Miquel, L. Mata-Cantero, E. Porras-De Francisco, Y.M. Chuang, H. Rubin, J.J. Lee, H. Eoh, J.S. Bader, E. Perez-Herran, A. Mendoza-Losana, and P.C. Karakousis, *Inhibiting the stringent response blocks Mycobacterium tuberculosis entry into quiescence and reduces persistence.* Sci Adv, 2019. **5**(3): p. eaav2104.

56. Bhaskar, A., C. De Piano, E. Gelman, J.D. McKinney, and N. Dhar, *Elucidating the role of (p) ppGpp in mycobacterial persistence against antibiotics.* IUBMB life, 2018. **70**(9): p. 836-844.

57. Conlon, B.P., S.E. Rowe, A.B. Gandt, A.S. Nuxoll, N.P. Donegan, E.A. Zalis, G. Clair, J.N. Adkins, A.L. Cheung, and K. Lewis, *Persister formation in Staphylococcus aureus is associated with ATP depletion.* Nature Microbiology, 2016. **1**(5): p. 16051.

58. Kapoor, G., S. Saigal, and A. Elongavan, *Action and resistance mechanisms of antibiotics: A guide for clinicians.* Journal of Anaesthesiology Clinical Pharmacology, 2017. **33**(3): p. 300-305.

773 59. Kohanski, M.A., D.J. Dwyer, B. Hayete, C.A. Lawrence, and J.J. Collins, *A common*
774 *mechanism of cellular death induced by bactericidal antibiotics.* Cell, 2007. **130**(5): p.
775 797-810.
776 60. Sebastian, J., S. Swaminath, R.R. Nair, K. Jakkala, A. Pradhan, and P. Ajitkumar, *De*
777 *Novo Emergence of Genetically Resistant Mutants of Mycobacterium tuberculosis from*
778 *the Persistence Phase Cells Formed against Antituberculosis Drugs In Vitro.* Antimicrob
779 Agents Chemother, 2017. **61**(2).

780

FIGURE 1

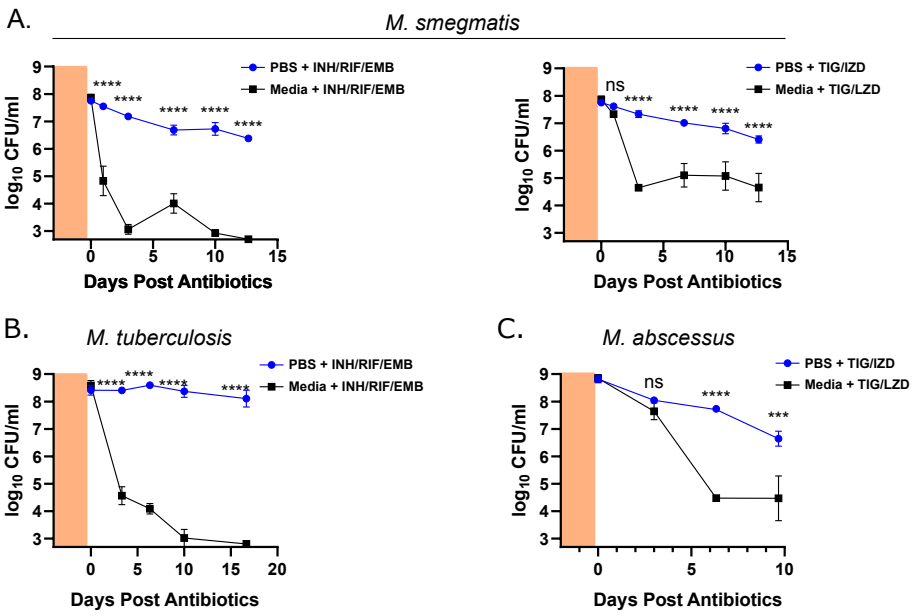
A.
M. smegmatis
PBS + INH/RIF/EMB
Media + INH/RIF/EMB
log10 CFU/ml
Days Post Antibiotics
PBS + TIG/IZD
Media + TIG/LZD
ns
B.
M. tuberculosis
C.
M. abscessus

FIGURE 2

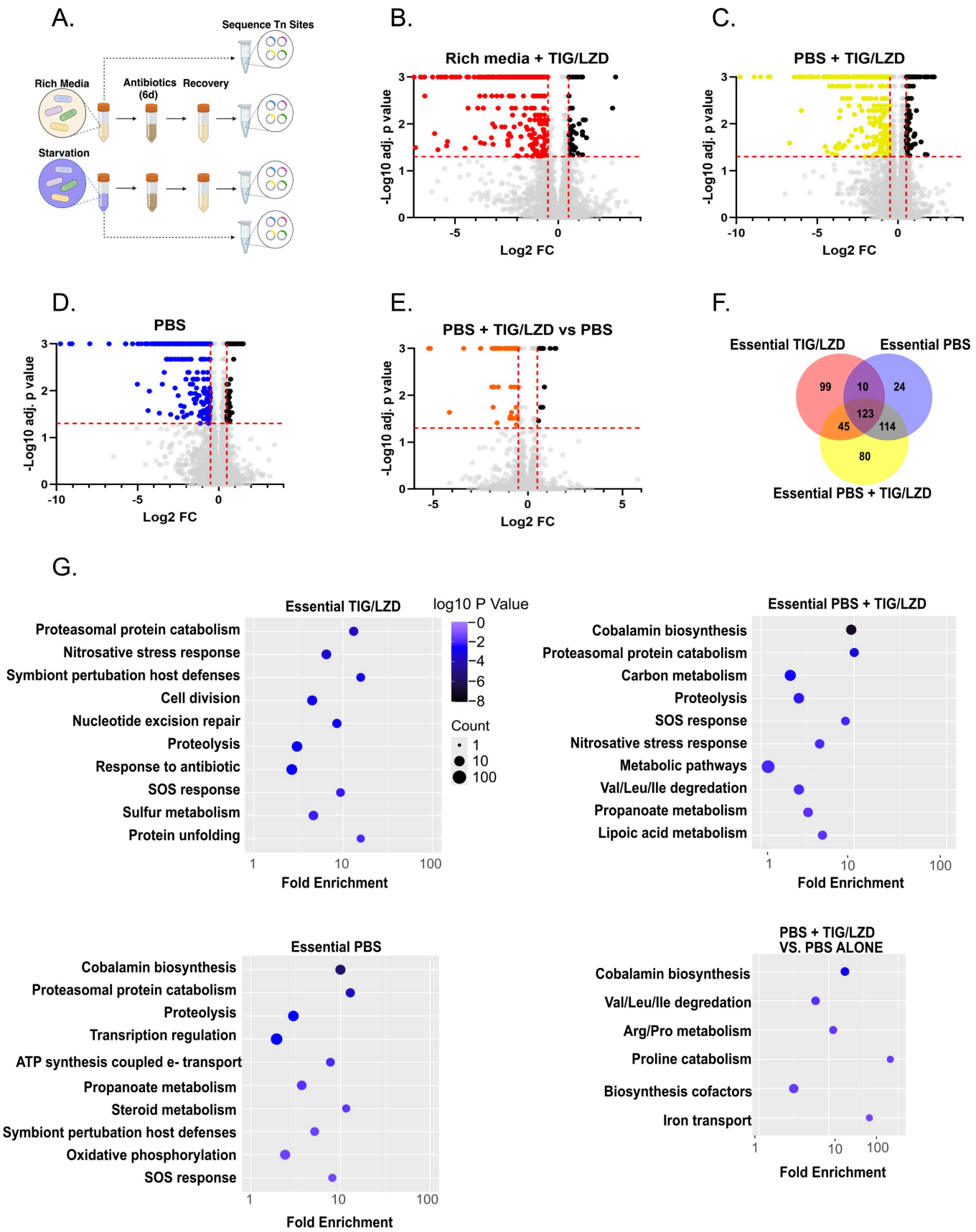
A.
Sequence Tn Sites
Rich Media
Antibiotics (6d)
Recovery
Starvation
B.
Rich media + TIG/LZD
-Log10 adj. p value
Log2 FC
C.
PBS + TIG/LZD
-Log10 adj. p value
Log2 FC
D.
PBS
-Log10 adj. p value
Log2 FC
E.
PBS + TIG/LZD vs PBS
-Log10 adj. p value
Log2 FC
F.
Essential TIG/LZD
Essential PBS
Essential PBS + TIG/LZD
99
10
24
123
45
114
80
G.
Essential TIG/LZD
log10 P Value
Count
Proteasomal protein catabolism
Nitrosative stress response
Symbiont pertubation host defenses
Cell division
Nucleotide excision repair
Proteolysis
Response to antibiotic
SOS response
Sulfur metabolism
Protein unfolding
Fold Enrichment
Essential PBS + TIG/LZD
Cobalamin biosynthesis
Proteasomal protein catabolism
Carbon metabolism
Proteolysis
SOS response
Nitrosative stress response
Metabolic pathways
Val/Leu/Ile degredation
Propanoate metabolism
Lipoic acid metabolism
Fold Enrichment
Essential PBS
Cobalamin biosynthesis
Proteasomal protein catabolism
Proteolysis
Transription regulation
ATP synthesis coupled e- transport
Propanoate metabolism
Steroid metabolism
Symbiont pertubation host defenses
Oxidative phosphorylation
SOS response
Fold Enrichment
PBS + TIG/LZD VS. PBS ALONE
Cobalamin biosynthesis
Val/Leu/Ile degredation
Arg/Pro metabolism
Proline catabolism
Biosynthesis cofactors
Iron transport
Fold Enrichment

FIGURE 3

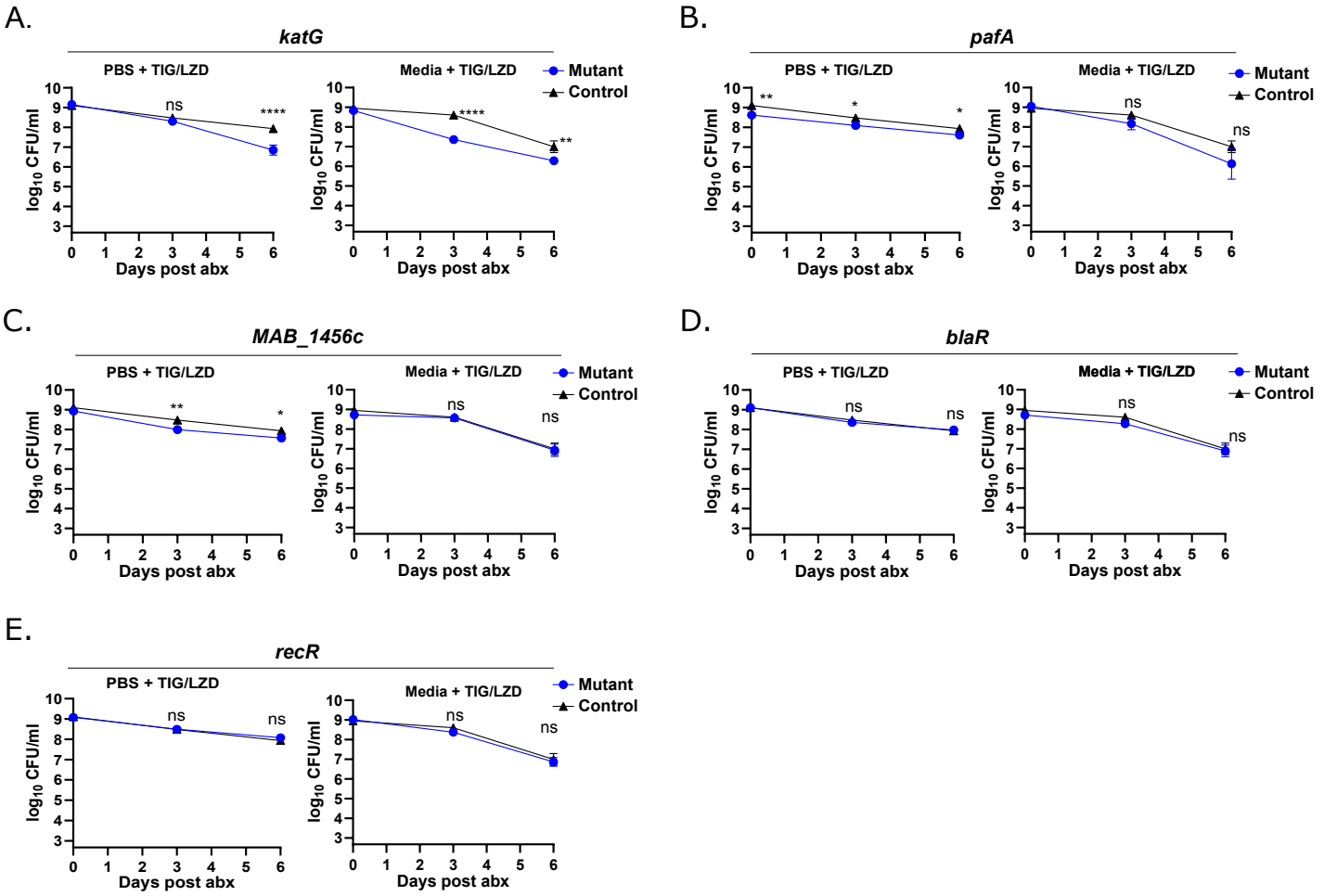
A.
katG
PBS + TIG/LZD
Media + TIG/LZD
Mutant
Control
log10 CFU/ml
Days post abx
ns
****
**
B.
pafA
PBS + TIG/LZD
Media + TIG/LZD
Mutant
Control
log10 CFU/ml
Days post abx
**
*
ns
C.
MAB_1456c
PBS + TIG/LZD
Media + TIG/LZD
Mutant
Control
log10 CFU/ml
Days post abx
**
*
ns
D.
blaR
PBS + TIG/LZD
Media + TIG/LZD
Mutant
Control
log10 CFU/ml
Days post abx
ns
E.
recR
PBS + TIG/LZD
Media + TIG/LZD
Mutant
Control
log10 CFU/ml
Days post abx
ns

FIGURE 4

A.

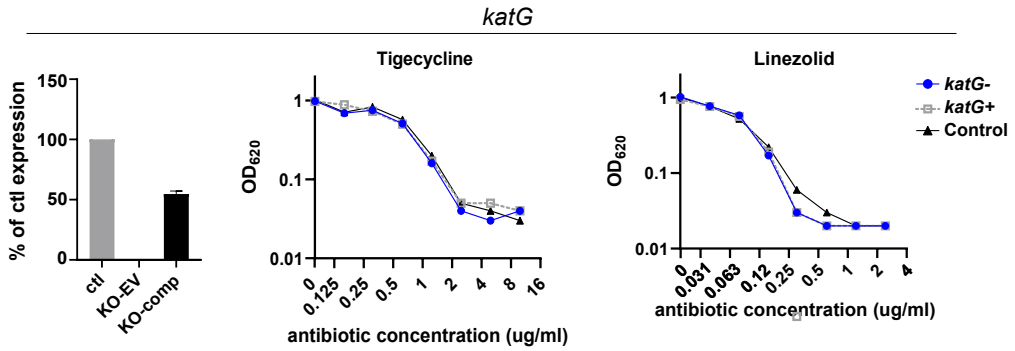

B.

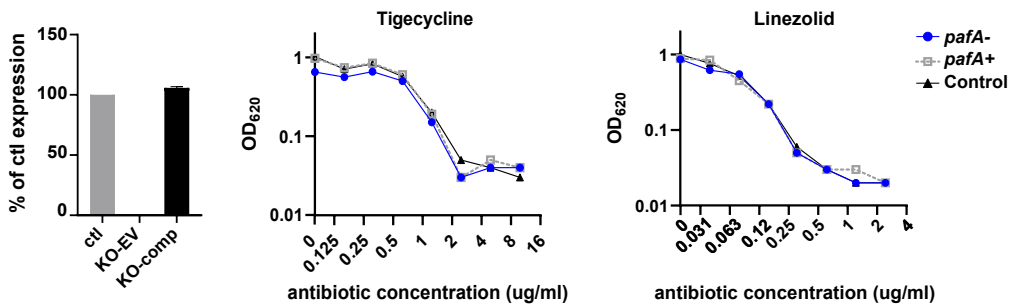

C.

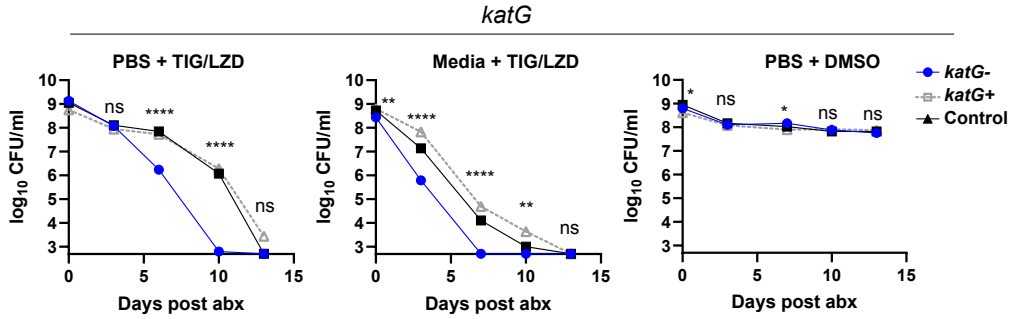

D.

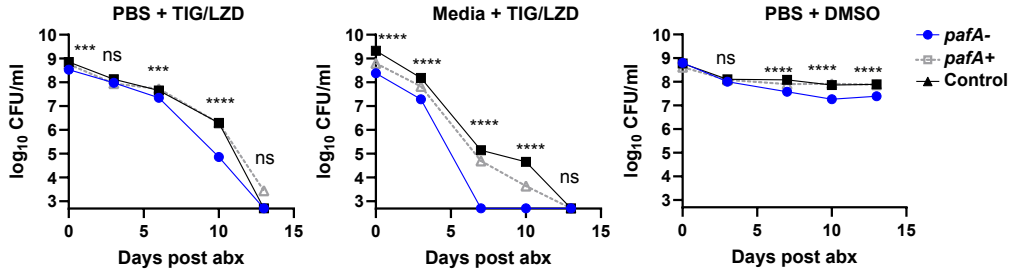

FIGURE 5

A.

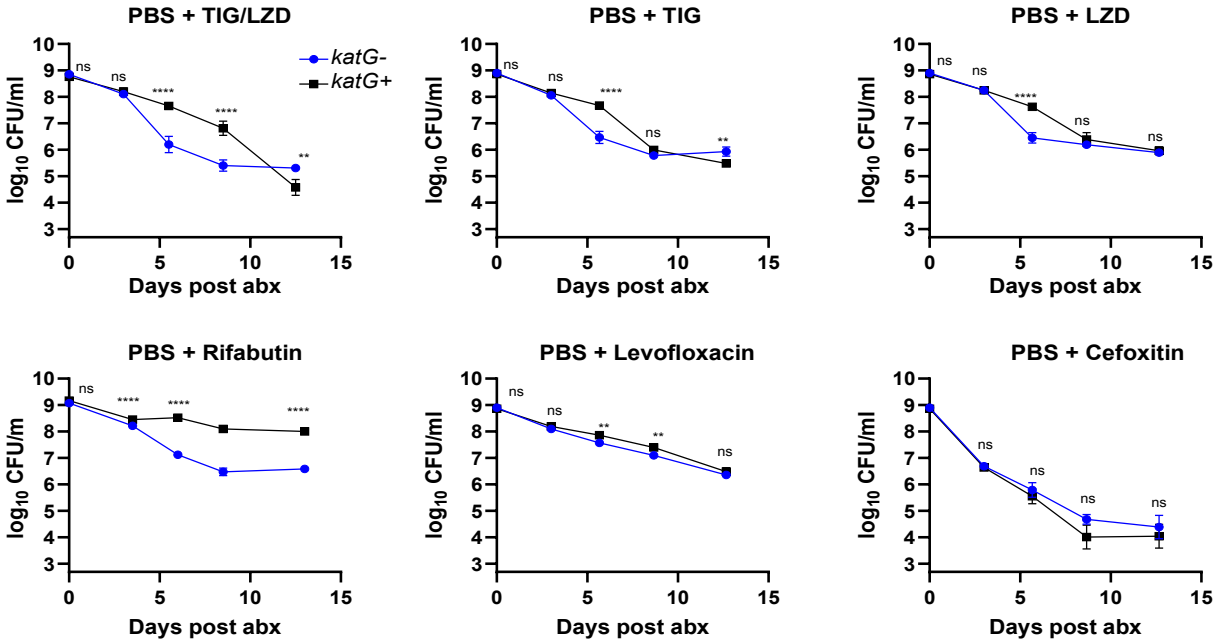
PBS + TIG/LZD
PBS + TIG
PBS + LZD
PBS + Rifabutin
PBS + Levofloxacin
PBS + Cefoxitin
katG-
katG+
log10 CFU/ml
Days post abx
ns
****
**

B.

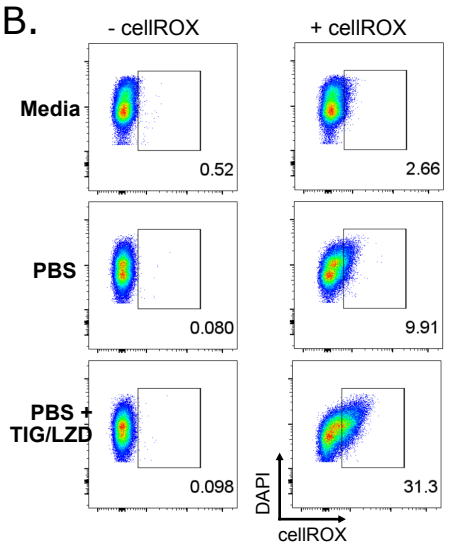
- cellROX
+ cellROX
Media
PBS
PBS + TIG/LZD
0.52
2.66
0.080
9.91
0.098
31.3
DAPI
cellROX

C.

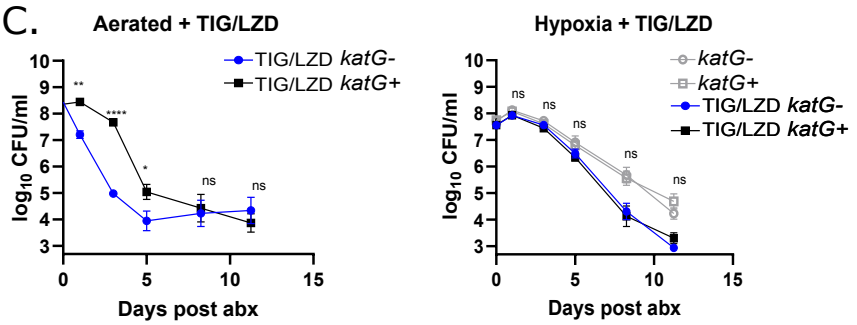
Aerated + TIG/LZD
Hypoxia + TIG/LZD
TIG/LZD katG-
TIG/LZD katG+
katG-
katG+
log10 CFU/ml
Days post abx
ns
*
**
****

FIGURE 6

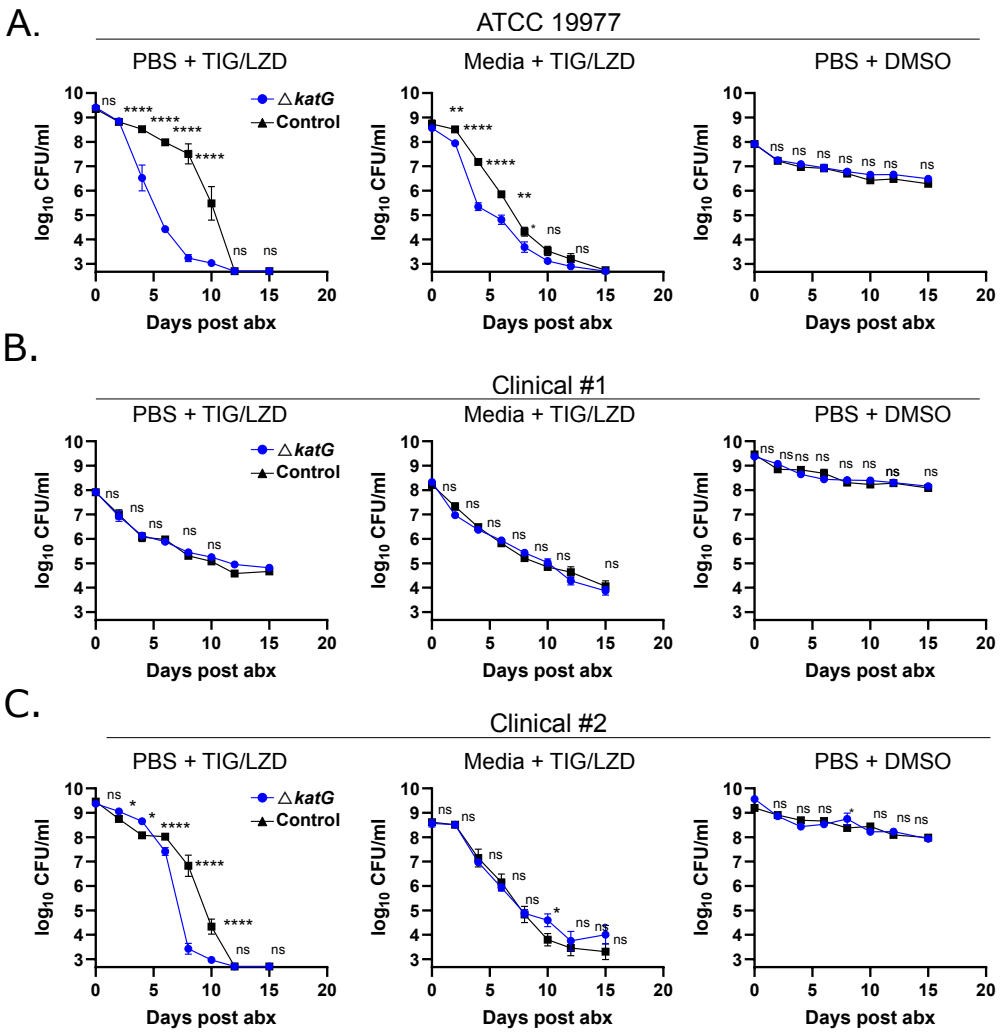
A.
ATCC 19977
PBS + TIG/LZD
Media + TIG/LZD
PBS + DMSO
△katG
Control
log10 CFU/ml
Days post abx
B.
Clinical #1
PBS + TIG/LZD
Media + TIG/LZD
PBS + DMSO
△katG
Control
log10 CFU/ml
Days post abx
C.
Clinical #2
PBS + TIG/LZD
Media + TIG/LZD
PBS + DMSO
△katG
Control
log10 CFU/ml
Days post abx

SUPPLEMENTAL FIGURE 1

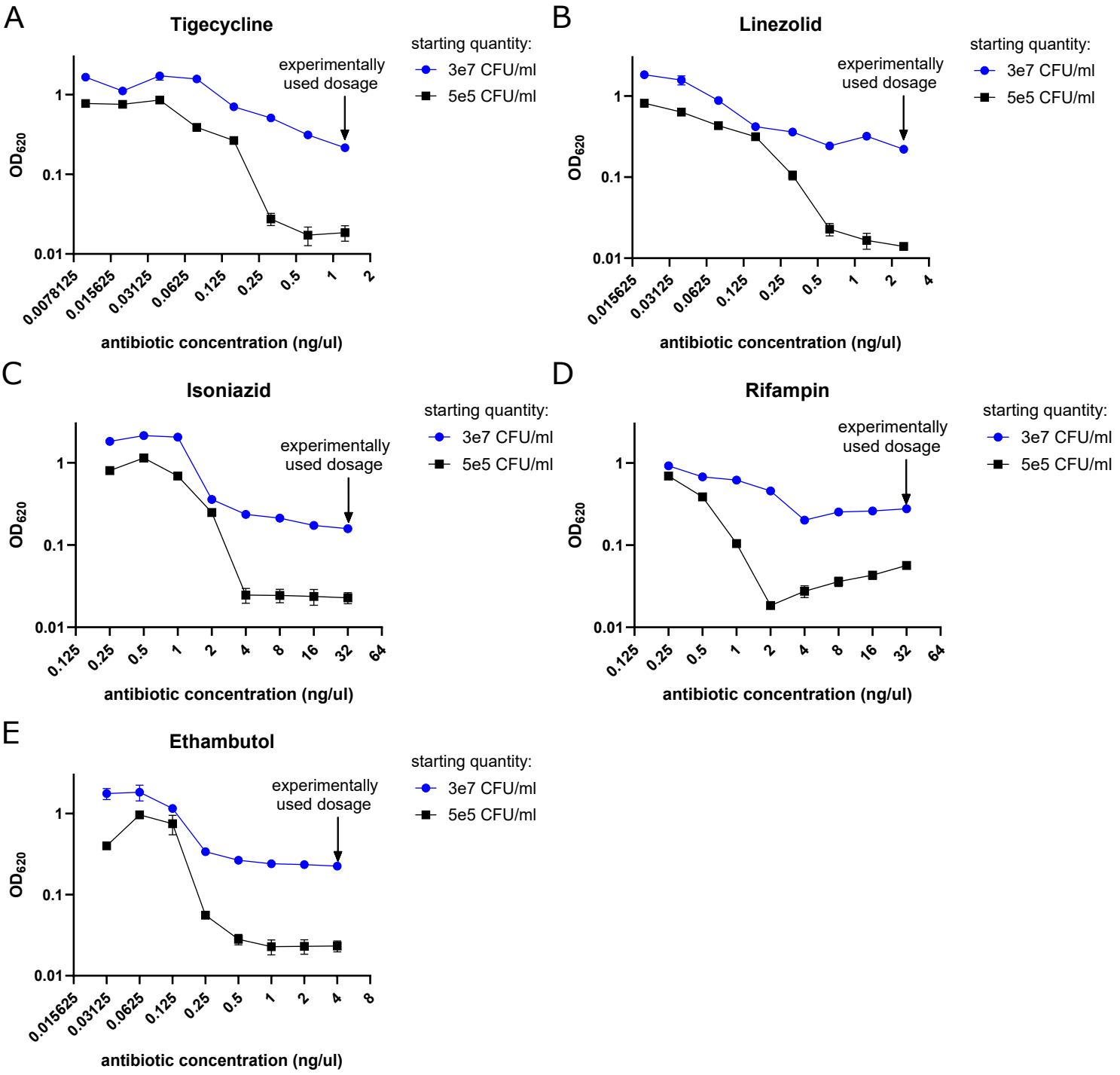

SUPPLEMENTAL FIGURE 2

A

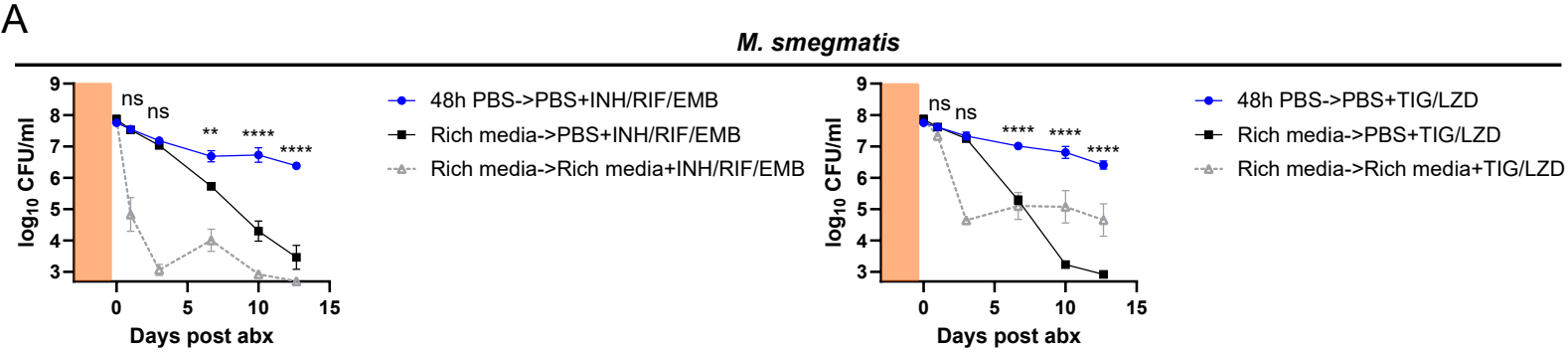

B

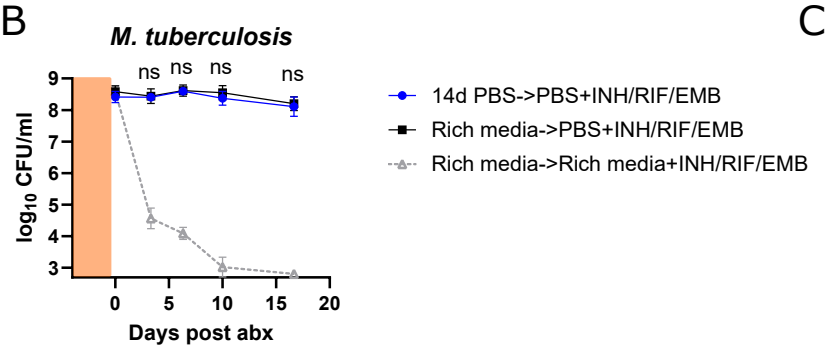
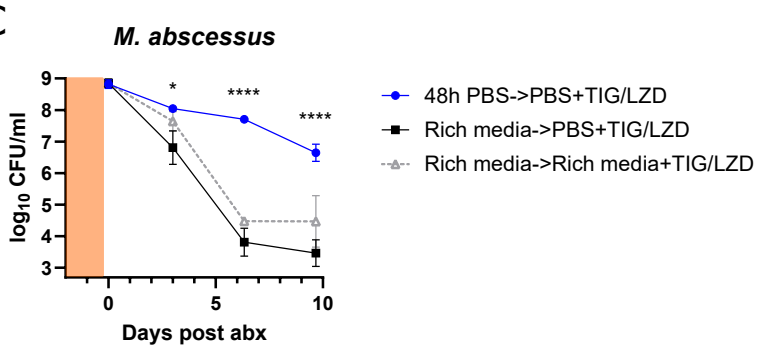
C